Detailed optical study of the transparent wing membranes of the dragonfly *Aeshna cyanea*

I. R. Hooper[1], P. Vukusic,[1] and R. J. Wootton[2]

[1]School of Physics, University of Exeter, Exeter, EX4 4QL, UK
[2]School of Biosciences, University of Exeter, Exeter, EX4 4PS
i.r.hooper@exeter.ac.uk

Abstract: The optical properties of transparent single membranes on the wings of the dragonfly *Aeshna cyanea* have been investigated. These membranes comprise one central thick cuticular layer covered dorsally and ventrally with typical odonatan wax pruinosity. Optical characterisation of individual membranes reveals they can support optical guided modes comprising differential polarisation reflection. We suggest this may offer an intraspecific signalling channel. The guided modes' characteristics depend on membrane thickness and the nature of the wax pruinosity. We accurately modelled multiple optical data sets simultaneously, thereby inaugurally quantifying the roughness of the pruinosity and the complex refractive indices of the wax and the odonatan cuticle.

©2006 Optical Society of America

OCIS codes: (310.2790) Guided Waves: (310.6860) Thin films, optical properties

References and Links

1. P. Vukusic, and J. R. Sambles, "Photonic structures in Biology," Nature **424**, 852-855 (2003).
2. P. Vukusic, J. R. Sambles, and C. R. Lawrence, "Structurally assisted blackness in butterfly scales," Proc. R. Soc. London Ser. B. (Suppl. i.e. Biology Letters) **271**, S237-S239 (2004).
3. R. J. Wootton, "The functional morphology of the wings of Odonata," Adv. in Odon. **5**, 153-169 (1991).
4. S. N. Gorb, A. Kesel, and J. Berger, "Microsculpture of the wing surface in Odonata: evidence for cuticular wax covering," Arthropod structure and development **29**, 129-135 (2000).
5. T. Wagner, C. Neinhuis, and W. Barthlott, "Wettability and contaminability of insect wings as a function of their surface sculptures," Acta Zoologica **77**, 213-225 (1996).
6. H. Ghiradella, and W. Radigan, "Collembolan cuticle: wax layer and anti-wetting properties," J. Insect Physio*l*. **20**, 301–306 (1974).
7. S. P. Sane, "The aerodynamics of insect flight," J. Exp. Biol. **206**, 4191-4208 (2003).
8. J. M. Wakeling, and C. P. Ellington, "Dragonfly flight," J. Exp. Biol. **200**, 543-556 (1997).
9. P. S. Corbet, *Dragonflies: behaviour and ecology of Odonata,* (Comstock Publishing Associates, Cornell University Press. 1999).
10. P. Vukusic, Natural Photonics, Physics World, Feb. 2004.
11. P. Vukusic, J. R. Sambles, and R. J. Wootton, "Remarkable iridescence in the hind-wings of the damselfly *Neurobasis chinensis* (Linnaeus) (Zygoptera Calopterygidae)," Proc. R. Soc. London Ser. B. **271**, 595-601 (2004).
12. T. Hariyama, M. Hironaka, H. Horiguchi, and D. G. Stavenga, "The Leaf Beetle, the Jewel Beetle and the Damselfly; Insects with a Multilayered Show Case" In *Structural Colors*, S. Yoshioka, S. and Kinoshita, eds. (Osaka University Press, Osaka, 2005), pp. 153-176.
13. L. Névot, and P. Croce, "Caractérisation des surfaces par réflexion rasante de rayons X. Application à l'étude du polissage de quelques verres silicates," Revue. Phys. Appl. **15**, 761-779 (1980).
14. P. K. Tien, "Integrated optics and new wave phenomena in optical waveguides," Rev. Mod. Phys. **49,** 361-420 (1977).
15. P. Vukusic, J. R. Sambles, C. R. Lawrence, and R. J. Wootton, "Quantified interference and diffraction in single Morpho butterfly scales," Proc. R. Soc. London Ser. B **266**, 1403-1411 (1999).
16. S. Liang, A. H. Strahler, X. Jin, and Q. Zhu, "Comparisons of Radiative transfer models of vegetation canopies and laboratory measurements," Remote Sens. Environ. **61**, 129-138 (1997).
17. Z. J. Wang, "Dissecting insect flight," Ann. Rev. Fluid Mech. **37**, 183-210 (2005).
18. J. Kim, "Control of turbulent boundary layers," Phys. Fluids **15**, 1093-1105 (2003).
19. M. Okamoto, K. Yasuda, and A. Azuma, "Aerodynamic characteristics of the wings and body of a dragonfly," J. Exp. Biol. **199**, 281-294 (1996).

20. A A. Barybin, and V. A. Dmitriev, *Modern Electrodynamics and Coupled-Mode Theory: Application to Guided-Wave Optics* (Rinton Press, Princeton, New Jersey, 2002).
21. A. S. Bonnet, G. Caloz, and F. Mahé, "Guided modes of integrated optical guides. A mathematical study," J. App. Maths **60**, 225-261 (1998).
22. E. P. Meyer, and T. Labhart, "Morphological specializations of dorsal rim ommatidia in the compound eye of dragonflies and damselflies (Odonata)," Cell and Tissue Research, **272**, 17–22. (1993).
23. T. Labhart ,and E. P. Meyer, "Detectors for polarized skylight in insects: a survey of ommatidial specializations in the dorsal rim area of the compound eye," Microscopy Research and Technique **47**, 368–379 (1999).
24. T. Cronin, N. Shashar, R. L. Caldwell, J. Marshall, A. G. Cheroske, and T. Chiou, "Polarization vision and its role in Biological signaling," Int. and Comp Biol. **43**, 549-558 (2003).

1. Introduction

The microstructure in and on the wings of insects is the subject of extensive interest. These structures have developed for various purposes: conspecific signalling through the production of structural colour [1, 2]; mechanical strength [3]; wing-surface anti-wetting and self-cleaning [4, 5, 6] and aerodynamic properties [7, 8]. Investigation of these structures allows both a better understanding of the host species' evolutionary development [3, 9] and reverse engineering of the structures to enable production of novel systems that perform similar tasks [10].

Odonatan wings generally comprise a framework of narrow veins, interconnected by a thin membrane to form small transparent windows 2 mm^2 or less in area. In some species, optically specialised wing membranes may be structurally coloured [11] and often pigmented with melanin [9]. Non-optically specialised transparent membranes consist of a cuticular layer, a few microns thick, between two much thinner superficial layers formed by cuticular wax (Fig. 1). Micro-sculpting in the wax layers forms the characteristic pruinosity associated with odonatan wing surfaces. This greatly reduces wetting of the wing surface by enhancing water droplet formation. Self cleaning then occurs when these droplets roll off the wing, taking micro- and macroscopic dust particles with them [4].
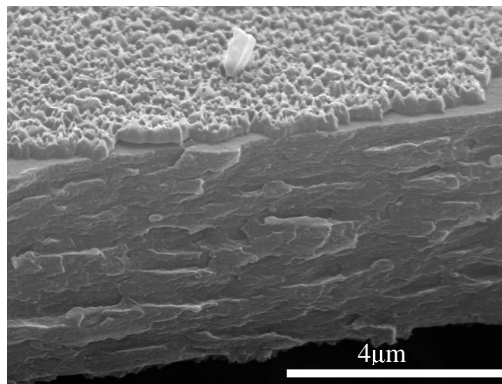

Fig. 1. An SEM image showing a cleaved section of the single wing membrane from the fore-wing of *Aeshna cyanea*. The thin wax pruinosity is visible as the rough overlayer on the top surface (scale bar: 2 µm).

The optical properties of odonatan wings have been the subject of only limited investigation and characterisation [10, 12]. Transparent wings in particular have not received the scientific attention that has been allocated to coloured wings. We have undertaken a detailed study of the transparency associated with many different insect wings. This paper describes the results of our investigation of one system; the transparent membranes that interconnect the network of wing venation of the dragonfly *Aeshna cyanea*. We report that these transparent membranes support leaky optical guided modes and that carefully fitting theory to experimental data yields the complex refractive indices and surface morphologies of

the wings. We describe the experimental and theoretical approach we have developed to achieve this optical characterisation and how it has led to the first detailed characterisation of the complex refractive index associated with cuticular wax layering.

2. Method

The transparent wings of several preserved male *Aeshna cyanea* dragonflies were examined using scanning and transmission electron microscopy (SEM and TEM). A Hitachi S-3200N electron microscope was used for SEM, the samples first cold-sputtered with 4 nm of gold. TEM analysis was undertaken after fixing samples in 3% glutaraldehyde at 21°C for 2 hours followed by rinsing in sodium cacodylate buffer. Subsequent fixing in 1% osmic acid in buffer for 1 hour was followed by block staining in 2% aqueous uranyl acetate for 1 hour, dehydration through an acetone series (ending with 100% acetone) and embedding in Spurr resin. Post microtomed sample sections were stained with lead citrate and examined using a JEOL 100S TEM instrument.
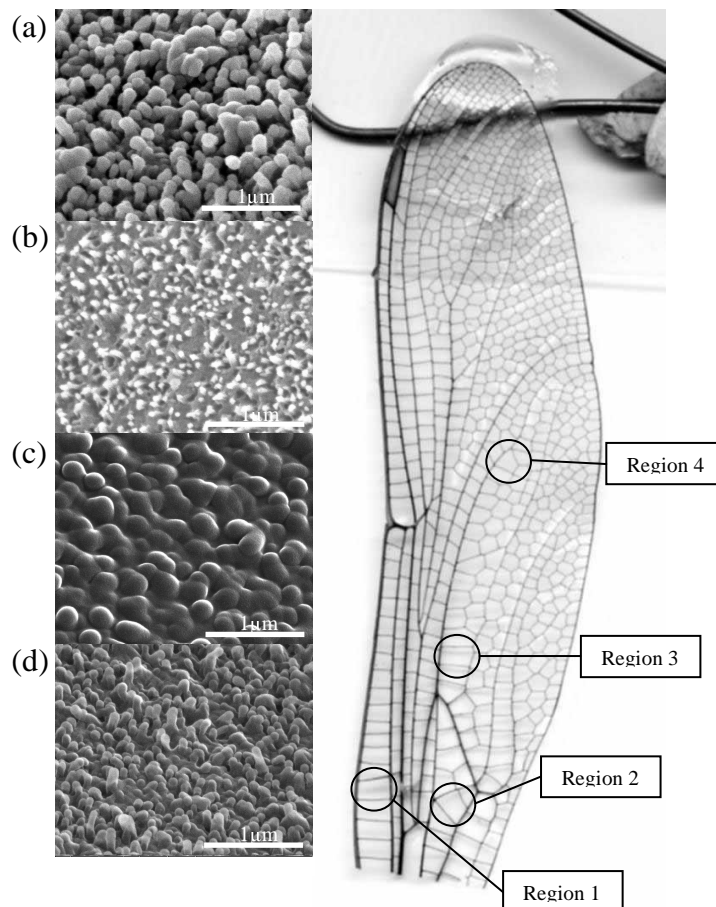

Fig. 2. A selection of SEM images, at the same magnification, of the surface cuticular wax layer from the *Aeshna cyanea* dragonfly wing shown on the right. (a) dorsal surface from region 1. (b) dorsal surface from region 2. (c) ventral surface from region 3. (d) dorsal surface from region 4. Although (c) is the only image which corresponds to the ventral surface, most other regions on the ventral surface resemble those of images (a) and (d).

Laser transmission measurements were conducted by mounting the specimens' right fore-wing onto a computer-driven rotating table on an optical bench. This enabled the incidence

angle of a laser to be changed accurately. Angle dependent transmission data was taken for TE- and TM- polarised light (at both 632.8 nm and 543 nm using HeNe lasers) from different individual membrane windows on the right fore-wing (Fig. 2). The laser was incident through an optical modulator (to enable phase sensitive detection to facilitate reduced noise), a polariser allowing only TE or TM linearly polarised light and a long focal length lens so the beam would pass solely through a single window within the wing. The transmitted laser light was collected with a photodiode optimised for phase sensitive detection. Absolute transmission was determined by ratioing these data against the intensity of the laser without the sample present.

One of the principle difficulties associated with modelling many-layer systems comprises overcoming degeneracies between layer thickness and refractive index. For this reason, multiple experimental data sets were simultaneously modelled using a multilayer optical code based upon recursive Fresnel formulae. In this code, individual single interface reflection (r) and transmission (t) amplitude coefficients were obtained for each interface within the multi-layer stack using the standard Fresnel formulae;

$$r_{ij} = \frac{k_{zi} - k_{zj}}{k_{zi} + k_{zj}} \tag{1}$$

$$t_{ij} = \frac{2k_{zi}}{k_{zi} + k_{zj}}$$

where the subscripts ij refer to the media on either side of the interface, k_{zi} and k_{zj} are the normal components of the wavevector of the incident and transmitted light given by $k_{zx} = k_0\sqrt{n_x^2 - n_1^2 \sin^2\theta_1}$, k_0 is the wavevector of the incident light, n_x is the refractive index of the medium in which the wavevector is being calculated, n_1 is the refractive index of the incident medium of the stack, and θ_1 is the angle of incidence of the light on the stack (measured from the normal to the interface of the first interface).

The effect of the roughness at the interfaces was modelled using the formalism of Névot and Croce. This gives a diminution factor for the individual single interface reflection and transmission amplitude coefficients, modelling the loss of power in the specular order due to scattering

$$r_{ij} = r_{ij}e^{-2k_{zi}k_{zj}\sigma^2} \text{ and } t_{ij} = t_{ij}e^{(k_{zi}-k_{zj})^2\sigma^2/2} \tag{2}$$

where σ measures the magnitude of the Gaussian roughness [13].

For the sort of roughness associated with the pruinosity on odonatan wings, however, due to its size and variation in shape, σ actually represents a measure of the amount of light scattered out of the specular beam. In this way, it is an indirect measure of the roughness itself, since it is the roughness which causes the scattering, but is not a direct measure of the average amplitude of the roughness as it is for smaller amplitude rough samples. Therefore, using Eq. (2) to modify the Fresnel amplitude coefficients, the entire structure's transmission amplitude coefficient from each wing region was calculated recursively using

$$t_{i,n} = \frac{t_{ij}t_{i+1,n}e^{2i\beta_i}}{1 + r_{ij}r_{i+1,n}e^{2i\beta_i}} \tag{3}$$

starting at the exit medium, with $\beta_i = k_{zi}d_i$, where d_i is the thickness of the ith layer and the subscript n corresponds to the exit medium. The transmission through the structure can then be calculated using

$$T = \text{Re}\left[\frac{k_{zn}}{k_{z1}}\right]tt^* \tag{4}$$

although in this case, since the wing is bounded by air on both sides, it is simply $T = tt^*$. All results obtained (eight datasets – two wavelengths for each of the four regions examined) were simultaneously fitted to theory using this model by an automated least squares reduction routine. All the parameters (the thickness and complex refractive indices of each layer, as well as the roughnesses of the surfaces) were allowed to vary freely between bounds which were determined by SEM and TEM (for the structural parameters) and previously published literature for typical values of the cuticle refractive index. The refractive index of odonatan cuticular wax, poorly documented in literature, was assumed to be between that of water (1.33) and that of cuticle (~1.56). The refractive indices of the cuticle and wax layers were forced to be the same for all regions (though different for the two wavelengths), and the structural parameters (the layer thickness, and the roughness parameter σ) were forced to be the same for the two wavelengths (though different for the four regions). By fitting the eight datasets simultaneously the degeneracy of the fitting was significantly reduced. The results and the corresponding fits are shown in Fig. 3. The parameters determined from the fitting are inset within the figure.
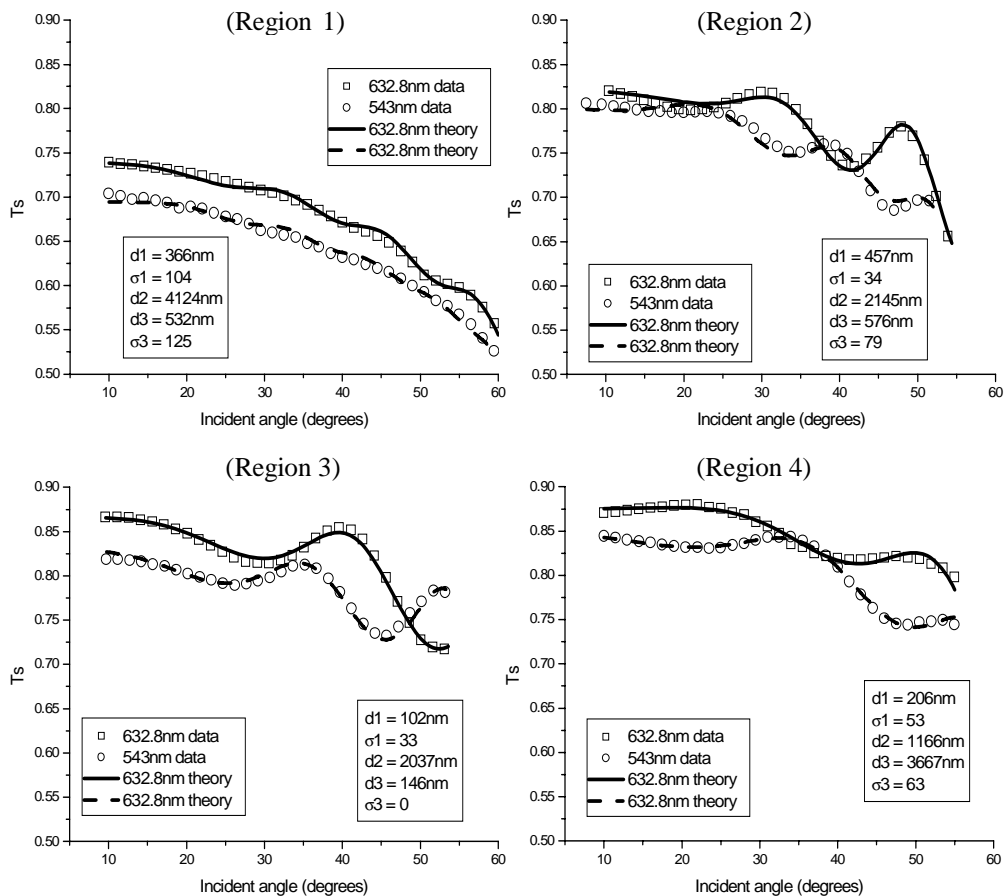

Fig. 3. Angle-dependent TE polarised transmission data and theoretical fits for the four regions investigated. These regions correspond to the windows in the wing shown in the photograph in Fig 2. d_1 is the thickness of the cuticular wax layer on the incident side of the structure, d_2 is the thickness of the bulk cuticle layer, and d_3 is the thickness of the cuticular wax layer on the exit side of the structure. σ_1 and σ_3 are the diminution constants describing the scattering due to the rough surfaces of the incident and exit interfaces respectively.

3. Results

The results in Fig. 3 show a series of fully leaky waveguide modes as minima in the angle-dependent transmission data. These occur due to constructive interference between reflections from the top and bottom interfaces of a layer within the multilayer stack [14], resulting in a partially trapped optical wave propagating within the cuticle layer. Since the reflections need to be coherent, the condition for their excitation is that the phase changes of the light upon reflection at the two interfaces, and upon propagation in the direction normal to the layer interfaces, result in the multiple reflections within the layer being in phase with each other. Power resonantly propagates along the waveguide (cuticle layer) when this condition is satisfied. The angular positions of the modes are determined both by the reflection coefficient at the interfaces of the multilayer stack (giving the phase change upon reflection of the light), and by the thickness and refractive index of the waveguiding layer (giving the phase change upon propagation within the layer). In general, the closer together the modes are in terms of angular position, the thicker the waveguiding layer. The term fully-leaky relates to the fact that the light incident on the interfaces of the waveguiding layer is only partially reflected allowing power to be 'leaked' into the transmitted or reflected orders (and in the case of rough interfaces into scattered light) in the media both above and below the waveguiding layer. This power loss results both in an increased width and decreased depth of the waveguide modes. It is clear, therefore, that the waveguide modes will be sensitive to the thickness of the layers, the refractive indices and any surface morphology in the layered system. Consequently, the parameters describing the system can be determined by fitting the experimental data to theory.

Simultaneous multi-dataset fitting yielded a value for the complex refractive index of the cuticle layer to be 1.56 ($\pm$ 0.01) + 0.003i ($\pm$ 0.001i). The imaginary part of this complex refractive index, which relates to the optical absorption in the system, is not zero as might be expected from totally transparent systems. However, it is an order of magnitude smaller than that previously measured in systems responsible for structural colour [15]. The refractive index of the dorsal and ventral layers of cuticular wax exhibited some dispersion and was determined to be 1.38 at 632.8 nm and 1.40 at 543 nm. These values are consistent with values cited for cuticular wax in plants [16]. The imaginary part of the refractive index of the cuticular wax, i.e. which relates to the optical absorption, could not be determined accurately. This is because the power loss to which it would normally be attributed is dominated in this instance by loss into the scattered light due to the pruinosity of the interface.

The σ values returned by the theoretical fits vary significantly both between regions and between dorsal and ventral sides of the structure. The supporting SEM images in Fig. 2 further indicate that not only does the magnitude of the surface roughness vary dramatically between regions, but so also does the form of the roughness.

4. Discussion

The amount of scattering from wavelength-scale features is dependent not only on the size of each feature, but also its general shape and refractive index. For this reason, the optical significance of the roughness associated with natural optical surfaces is only partially described by Gaussian formalism. In addition to the statistical pitch and amplitude, the shape and curvature of the microstructure also carry optical significance; i.e. a more rounded object is less likely to scatter electromagnetic radiation. In spite of this complexity, the σ values obtained from the theoretical fitting described here show a quantitative correlation to the nature of the surface roughness imaged by SEM. Smaller σ values ($\sigma < 35$) correspond to membrane regions with roughness of a smaller magnitude, or regions with significantly more rounded roughness. Higher value σ regions ($\sigma > 100$) are consistent with larger and less rounded surface roughness which delivers significantly more scattering. This accounts for the zero σ value obtained for the ventral surface of region 3. Here the cuticular wax has a very rounded form, and hence produces very little scattering (the much rougher dorsal surface dominates the scattering resulting in the zero value obtained)

The variability in the scale and type of the roughness from membrane regions on different parts of each characterised wing is curious. If the function of this roughness, combined with the hydrophobicity of wax, were solely anti-wetting (and consequently self-cleaning) one might be assume that all regions of the wing should have similar surface pruinosity because there would be an optimal scale of the roughness necessary for this purpose. The fact that this is clearly not the case might imply there may be a secondary function to this surface morphology. One potential candidate for this relates to aerodynamic surface drag; specifically control of the wing surface boundary layer [17, 18, 19]. Closer consideration of the scale of the membranes' surface roughness, however, and the significantly larger size of the wing venation makes this very unlikely (C. P. Ellington, private correspondence).

Leaky guided modes in natural layered systems, such as those revealed in this study, have not been reported previously. They are brought about by the propagation of incident light in the plane of the wing membrane. They are electromagnetic wave configurations which are solutions to Maxwell's equations and which conform to the physical conditions at membranes' surfaces. They form an extremely well known and widely studied field of technological photonics [20, 21]. Their existence in these transparent wing membranes is entirely predictable, although the effect of surface roughness is less straightforward to model. In this wing system, the presence of guided modes facilitates the differential reflection of each linear polarisation; under certain circumstances by as much as 30% at incidence angles around 45° and up to 60% at much higher angles (Vukusic, unpublished data). The biological relevance of such differential polarisation transmission, and hence differential polarisation reflection, is unknown. Certainly the dorsal rim area of the *Aeshna cyanea* compound eye appears anatomically specialized, its ommatidia comprising rhabdoms with only two, orthogonally-arranged, microvillar orientations [22]. In other species, this structure is directly responsible for polarization sensitive vision [23]: as such, it can be incorporated into high-level visual perception in a manner akin to colour vision [24]. Despite this specialisation appearing somewhat limited to the dorsal rim area, and hence ideally suited for celestial navigation, it is nonetheless possible the polarisation vision sensitivity of *Aeshna cyanea* may also be utilized for one or more tasks other than navigation. Object recognition, contrast enhancement, and signal detection and discrimination would number among these tasks. Signal detection would in this case appear to be a property that is complementary to the actual production of polarised signals from the transparent wing membranes themselves. It would be interesting to investigate whether our human perception of the apparently featureless transparency of these odonatan wings actually overlooks its effectiveness as an extremely simple polarisation signalling channel.

5. Conclusions

In this study a multi-variable optical fitting method has been designed and used to obtain the refractive index and micro-roughness scattering characteristics of material layers within various regions of a transparent *Aeshna cyanea* dragonfly wing membrane. The results suggest that the cuticular wax layers on the top and bottom surfaces of the wing have a wavelength-dependent refractive index of between 1.38 - 1.40. The fitting methodology identified a significant variation in the scale and form of the membrane surface roughness from different regions of wing. Though a preliminary quantification of this surface roughness has been made, improved surface roughness models will permit more accurate mathematical representation of the range and form of the surface structure that was encountered. While we identify the distinct presence of variation in wing-membrane surface roughness in this paper, the purpose of the variation itself is unknown.

Finally, we identified and characterised a differential reflection of polarised light from the wing. We suggest that this may complement the specialised polarisation sensitivity associated with *Aeshna cyanea* and other odonatan vision which has been described by other workers.